

Natural Rubber with Low Heat Generation Achieved by the Inclusion of Boron Carbide

Gengsheng Weng, Guangsu Huang, Liangliang Qu, Peng Zhang, Yijing Nie, Jingrong Wu

State Key Laboratory of Polymer Material Engineering, College of Polymer Science and Engineering, Sichuan University, Chengdu, 610065, People's Republic of China

Received 20 September 2009; accepted 24 February 2010

DOI 10.1002/app.32336

Published online 10 June 2010 in Wiley InterScience (www.interscience.wiley.com).

ABSTRACT: Natural rubber with low heat generation was prepared by the inclusion of boron carbide (B_4C). Tensile testing, scanning electron microscopy (SEM), dynamic mechanical analysis, and thermal constant analysis were performed. The results show that a slight deterioration of tensile strength only occurred at a high volume content (>20 vol %). The thermal conductivity increased for the formation of well-maintained B_4C thermal conductive pathways. SEM images and theoretical

analysis demonstrated that the specific area of B_4C was small and the interfacial activity was low. Infrared thermal images taken by the infrared camera proved the low heat generation of the composites, which originated from the high thermal conductivity and the weak interface. © 2010 Wiley Periodicals, Inc. *J Appl Polym Sci* 118: 2050–2055, 2010

Key words: composites; elastomers; thermal properties

INTRODUCTION

Heat generated from the cyclic deformation of rubbers at sufficient magnitudes of amplitude and frequency cannot be easily conducted away; this results in an increasing temperature for the rubber components. High temperatures accelerate the fatigue of rubbers, so it is very important to find proper ways to reduce the heat buildup of rubbers in dynamic applications.^{1,2} Heat generation mainly originates from the viscoelasticity of rubbers, and it increases with increases in hysteresis loss, frequency, stroke, and ambient temperature.^{3,4} The inclusion of fillers in rubbers can significantly affect the heat generation by filler loading, thermal conductivity, interfacial interaction, and the shape and dimension of fillers. So, the formation of thermal conductive pathways in a rubber matrix with a high thermal conductivity can be helpful to attenuate heat buildup. Meanwhile, fillers with a small specific area and relative weak interfacial activity can also reduce the quantity of heat generated in cyclic loadings. Many studies have been reported on the heat buildup of rubbers, but most of the fillers investigated have been conventional fillers, such as carbon black and silica.^{5–7} In this study, we

chose boron carbide (B_4C) as a thermal conductive filler to obtain natural rubber (NR) composites with low heat buildup, as proven by the use of an infrared camera. These B_4C -filled NR composites could also be used as thermal neutron radiation shields for the high value of the neutron cross section of boron.⁸

EXPERIMENTAL

The NR used in this study (SMR 1) was purchased from Mengwang Rubber Corp. (Shanghai, China). Nonvulcanized NR, which contained all of the vulcanization ingredients, was prepared in a laboratory twin-roll mixing mill (SK-160B, Shanghai Rubber Machine Co., Shanghai, China) at room temperature and was then vulcanized at 140°C for 10 min under a pressure of 1.5×10^7 Pa. We prepared composites with different volume contents of B_4C (Sidi Chemistry Co., Chengdu, Sichuan, China) from 0 to 45 vol %. The morphology of the composites was observed by scanning electron microscopy (SEM; The Standard of Japanese Electrical Manufacture's Association (JEM), JSM 5900LV (Infrared camera: FLIR Systems, Boston, MA)). The tensile performances were measured by an Instron 5567 material testing machine (University Ave, Norwood, MA) (Japan Electronics Co., Ltd. (JEOL), 1-2, Musashino 3-chome Akishima Tokyo, Japan) in tensile mode with a load cell with a 1-kN capacity. The specimen was a dumbbell-shaped thin strip ($25 \times 4 \times 2$ mm³), and the experiments were performed at a tensile speed of 500 mm/min. The nonlinear viscoelasticity of the B_4C /NR composites (Payne effect) was tested by means of a TA Q800 instrument (New Castle, DE) with a frequency of 1 Hz and amplitudes ranging from 0 to

Correspondence to: G. Huang (guangsu-huang@hotmail.com).

Contract grant sponsor: Major State Basic Research Projects of China; contract grant number: 50673059.

Contract grant sponsor: National Nature Science Foundation of China; contract grant number: 50103007.

7500 μm at a temperature of 25°C in tensile mode. The rectangular specimens had a thickness of 1 mm, a width of 6 mm, and a length of 40 mm. The thermal conductivity of the composites was measured by hot disk thermal constant analyzers (model 2500 (Hot disk thermal constant analyzers: K-analys, Salagatan, Uppsala, Sweden)) at a temperature of 25°C. An infrared camera (ThermoVision A20) was used to test the heat buildup of the $\text{B}_4\text{C}/\text{NR}$ composites at room temperature. Cylindrical rubber specimens (24 mm in height and 49 mm in diameter) were subjected to cyclic compression with an MTS 810 material test machine (Mechanical Testing & Simulation (MTS) Systems Corporation, Technology Drive, Eden Prairie, MN). The frequency of loading was 5 Hz, and the amplitude was 3.5 mm. The test procedures were terminated when the sample was tested for about 40 min.

RESULTS AND DISCUSSION

Morphological and mechanical features

The morphologies of the $\text{B}_4\text{C}/\text{NR}$ composite with different volume contents are shown in Figure 1.

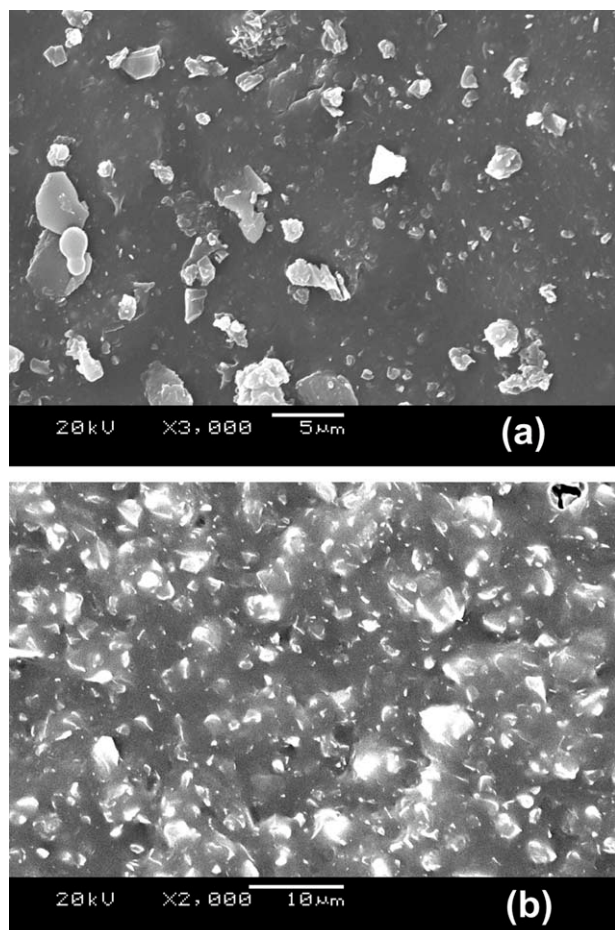


Figure 1 SEM micrographs of $\text{B}_4\text{C}/\text{NR}$ composites with different volume contents: (a) 14 and (b) 40 vol % B_4C -filled NR.

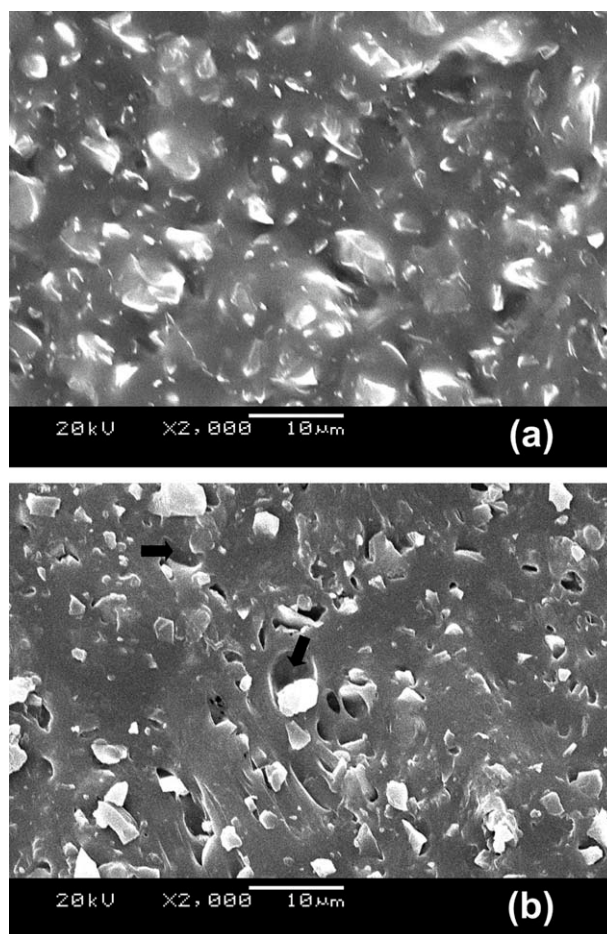


Figure 2 SEM micrographs of the 30 vol % $\text{B}_4\text{C}/\text{NR}$ composite (a) before and (b) after cyclic compression testing.

The diameter of B_4C particles was about 2–5 μm . The B_4C particles were homogeneously dispersed at all ranges of volume content. Particularly, cavities appeared at a high content [Fig. 1(b)], which indicated the relatively weak interaction between B_4C and NR. This was also proven by the SEM images shown in Figure 2. This means that more cavities appeared and some B_4C particles were pulled off after the cyclic compression test [see the regions in Fig. 2(b) indicated by the black arrows] because of the weak interfacial interaction. The tensile strength variation of the $\text{B}_4\text{C}/\text{NR}$ composites is plotted in Figure 3. The enhancement of the tensile strength at a content range of 3–20 vol % confirmed the well-maintained B_4C network at low contents. At high volume contents, the tensile strength decreased; this was attributed to the structural rupture of the B_4C network during elongation.

To reveal the structural changes in the filler network, the Payne effect was investigated by the measurement of the dynamic amplitude scanning at a frequency of 1 Hz.^{9–11} This nonlinear behavior in the nondestructive regime of the filled rubbers has been regarded as an important subject in numerous studies on filler structure and matrix–filler interactions.¹² The

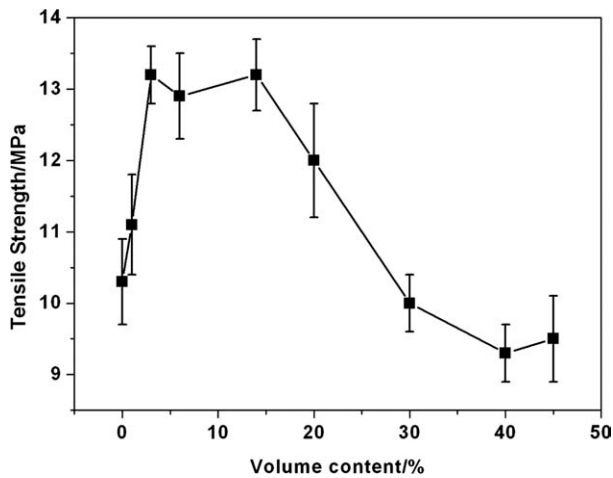


Figure 3 Tensile strength of the B₄C/NR composites as a function of the B₄C volume content.

storage modulus (G'), measured for composites with various levels of B₄C, is displayed in Figure 4(a). At low and intermediate contents of B₄C (0–14 vol %), G' exhibited an invariance in strain amplitudes for strains less than about 1%; this clearly suggests that the B₄C network existed at low strains. The invariance was not maintained at high B₄C contents because G' decreased even at very low strains. Corresponding $\tan \delta$ curves are plotted in Figure 4(b). Clearly, a maximum in the strain range was well established as a reflection of the significant hysteresis arising from the breakup of the filler network at high B₄C contents (>20 vol %).^{13–15} So, we concluded that a well-maintained filler network was achieved under a wide filler content range (0–20 vol %).

Thermal conductive network

The state of filler distribution is important. As described by the percolation theory, the enhancement of thermal conductivity is based on the continuous heat-conduction path formed by fillers.¹⁶ This was confirmed by the SEM images in Figure 1. Figure 5 shows the thermal conductivity as a function of the B₄C volume content. The thermal conductivity increased with B₄C loading. It reached a value of 0.76 W m⁻¹ K⁻¹ at a B₄C volume content of 45 vol %. To evaluate the enhancement of the thermal conductivity of the B₄C/NR composites, two theoretical models (Maxwell and Bruggeman) were used to predict the thermal conductivity, as shown in Figure 5¹⁷:

$$\text{Maxwell: } k = K_p \frac{K_f + 2K_p - 2V_f(K_p - K_f)}{K_f + 2K_p + V_f(K_p - K_f)} \quad (1)$$

$$\text{Bruggeman: } 1 - V_f = \frac{K_f - k}{K_f - K_p} \left(\frac{K_p}{k} \right)^{1/3} \quad (2)$$

where k is the thermal conductivity of the composite; K_f and K_p are the thermal conductivities of the filler

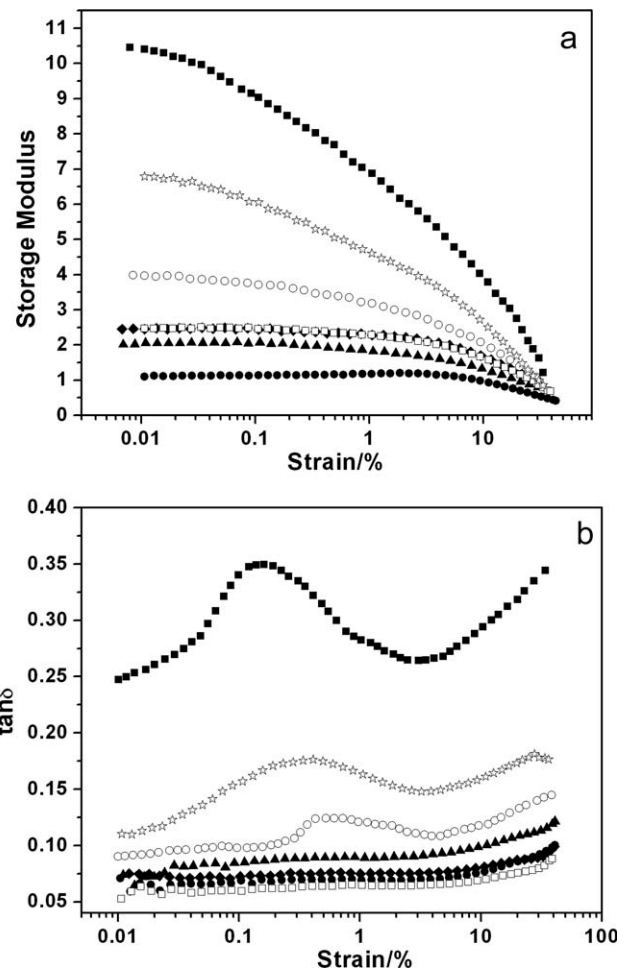


Figure 4 (a) G' and (b) $\tan \delta$ measured as a function of strain and with six different filler volume contents: (●) neat and (▲) 3, (◆) 6, (□) 14, (○) 20, (☆) 30, and (■) 40 vol %.

and polymer matrix, respectively; and V_f is the volume content of filler. The thermal conductivity of B₄C used here was 42 W/m K.¹⁸

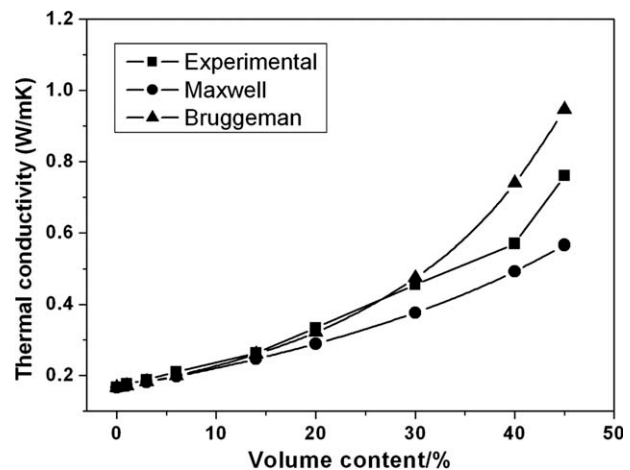


Figure 5 Comparison of the experimental thermal conductivity values of B₄C-filled NR with the theoretically predicted values.

As shown in Figure 5, the prediction of the Maxwell model deviated from the experimental data, whereas the prediction of the Bruggeman model was consistent with our experimental data at volume contents lower than 30 vol %, with only a slight overestimation at B₄C loadings greater than 30 vol %. That is, an ideal thermally conductive B₄C network pervading the matrix formed. It was the weak interfacial interaction that attenuated the thermal conductivity at high B₄C loadings, which was proved by Figures 1 and 2. A probable reason for the deviation of the Maxwell model is that it is an exact solution only for the effective conductivity of randomly distributed and noninteracting fillers in a continuous matrix. It does not take into account the interaction of the fillers.^{19,20} So, more exact theoretical models were developed to describe the mixing role of two-phase composite systems. Agari and co-workers^{21,22} proposed an important model to predict the thermal conductivity [eq. (3)], which is based on the generalization of models for parallel and series conduction in composites. According to the effective medium theory, Bruggeman^{20,23} reported a model by considering the neighboring particles as the incremental dispersed particles and the existing composite as the surrounding medium at each stage and, then, the integration of the thermal conductivity [eq. (4)]. Taking both the effect of interfacial thermal barrier resistance and particle shapes into consideration, Wang and Su²⁴ proposed a modified Bruggeman model [eq. (5)] to predict the thermal conductivity. By fitting the experimental data with the Agari and modified Bruggeman models, we obtained more information about the mechanism of thermal conduction (Fig. 6):

$$\text{Agari: } \log k = V_f C_2 \log K_f + V_p \log(C_1 K_p) \quad (3)$$

$$\text{Bruggeman: } 1 - V_f = \left(\frac{K_p}{k}\right)^{1/3} \left(\frac{K_f - k}{K_f - K_p}\right) \quad (4)$$

Modified Bruggeman:

$$(1 - V_f)^n = \left(\frac{K_p}{k}\right) \left(\frac{k - K_f(1 - \alpha)}{K_p - K_f(1 - \alpha)}\right)^n, \quad \alpha = a_k/a, \quad (5)$$

$$R_k = a_k/K_p, \quad n = 3/\Psi$$

In the Agari model, represented by eq. (3), V_p is the volume content of the polymer matrix, C_1 is related to the crystallinity and crystallite size of the matrix, and C_2 is related to the likelihood of the formation of connected filler thermal pathways. This model is also effective at high volume contents.^{21,22} The values of C_1 and C_2 should be between 0 and 1. A more easily conductive filler network can be formed in the composite when the C_2 value is close to 1. By data fitting, values of 0.1 and 0.9 were obtained for C_1

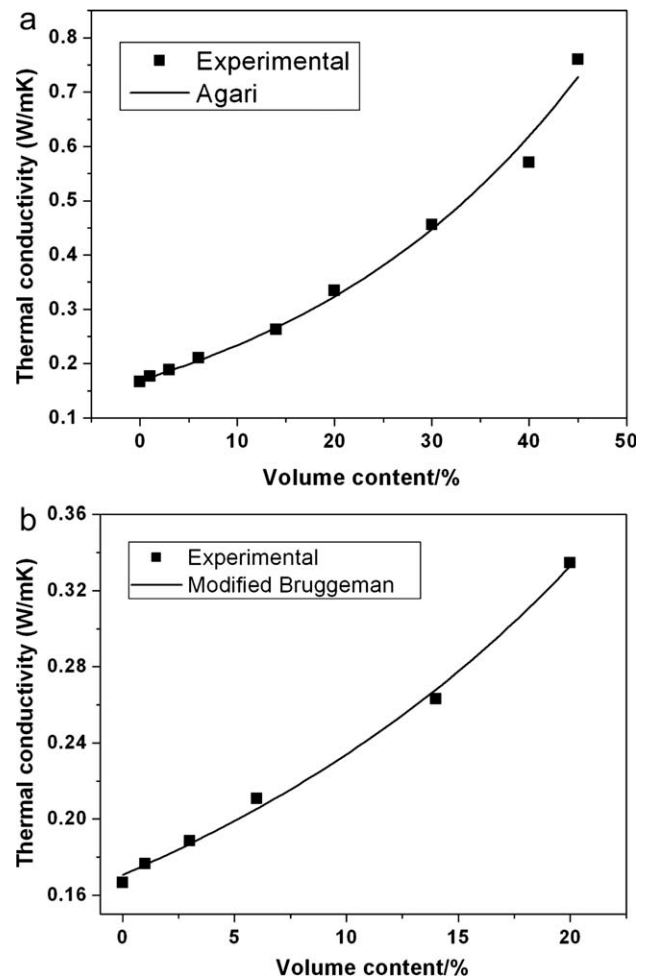


Figure 6 Experimental data of the thermal conductivity and curves fitted by the Agari and modified Bruggeman equations.

and C_2 . The C_2 value suggested that effective conductive bridges in the composite were formed. This was consistent with the dynamic mechanical measurement discussed previously.

The modified Bruggeman model further reflects the shape of filler and interfacial condition between the filler and matrix. In eq. (5), α is the interfacial thermal barrier resistance factor, n is particle shape factor, and Ψ is particle sphericity. The particle radius (a) here was verified by the scanning electron micrographs represented previously as having a value of 2 μm . The parameters a_K and R_K indicate the Kapitza radius and Kapitza resistance (interfacial thermal barrier resistance), respectively.²⁴ Taking into consideration the fact that filler agglomeration leads to the deviation of this model, we used data only at in range 0–20 vol % for fitting. The fitting results show that $n = 2.99$, $a_K = 1.04 \times 10^{-6}$ m, and $R_K = 6.4 \times 10^{-6}$ m² K/W. The value of n suggested that the specific area of the B₄C particles was small. The relatively high Kapitza resistance was mainly

derived from the poor interaction between B_4C and NR, which was proven by the SEM images. According to a survey of the literature, the dramatic enhancement of thermal conductivity occurs mainly within the region where R_K is less than $10^{-7} \text{ m}^2 \text{ K/W}$. When R_K is greater than $10^{-7} \text{ m}^2 \text{ K/W}$, the effect of Kapitza resistance on the thermal conductivity is quite low.^{25–27} So, we concluded that the dominating factor of thermal conductivity was the quality of the connected B_4C thermal pathways formed in the NR matrix.

Heat buildup under cyclic loading

To investigate the heat generation of the composites, an infrared camera was used to test the temperature increase at a temperature of 30°C . Figure 7 shows the infrared images taken at different times, which reveals that temperature increased very quickly. To illustrate the trends of heat generation, the values of heat buildup are plotted against time in Figure 8. This figure indicates that at volume contents of 0–14 vol %, the temperature variation (ΔT) was even lower than that of unfilled NR. When volume content increased further, ΔT increased dramatically; this resulted from the serious breakup of the B_4C network and largely increased the interfacial friction. Compared that of the 14 vol % carbon-black-filled NR system, the heat buildup in the B_4C -filled system was quite low. So, the appropriate filling of B_4C would benefit the heat dissipation in the dynamic application of rubbers.

To understand the mechanism of heat dissipation, we paid much attention to the main features of B_4C -filled NR, which possibly had great impact on the

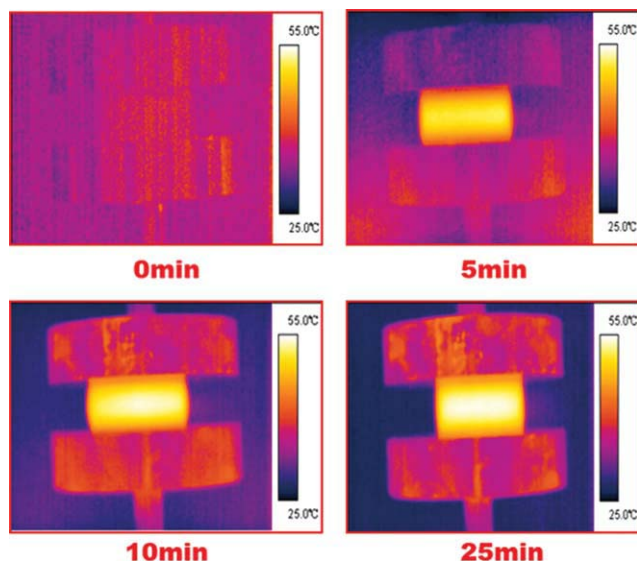


Figure 7 Images taken by infrared photography at different times. [Color figure can be viewed in the online issue, which is available at www.interscience.wiley.com.]

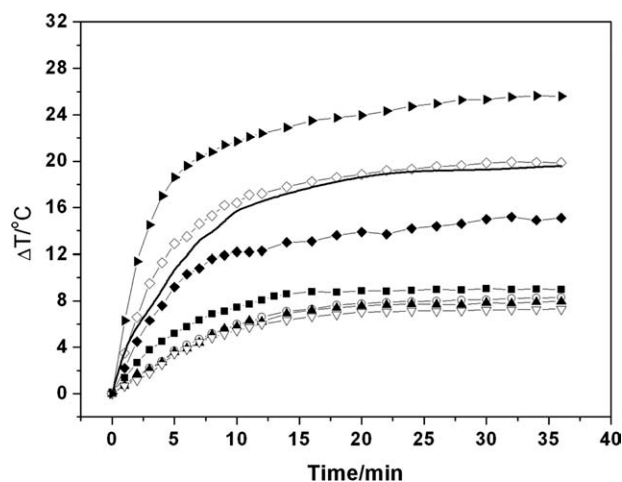


Figure 8 Heat buildup at a temperature of 30°C as a function of compression time. The ΔT values are indexed as follows: (■) neat and (○) 3, (▲) 6, (▽) 14, (◆) 20, (◇) 30, and (▶) 40 vol %. The solid straight line is the heat buildup curve of 14 vol % carbon-black (N770)-filled NR for comparison.

heat buildup of the composites. These main features included the (1) high thermal conductivity, (2) relatively weak interaction between B_4C and the NR matrix, and (3) small specific area of B_4C . Particularly, the thermal conductivity achieved theoretical values at a wide range of B_4C loadings for the satisfying thermal pathways formed in the NR matrix. This was an important way to attenuate the heat generation. In this study, the interfacial properties of B_4C were also very important for heat dissipation. On the one hand, the relatively small specific area of B_4C reduced the contact area; thus, the friction between the filler and matrix was reduced. On the other hand, because of the weak interfacial interaction, we concluded that there was no glassy bridges, which was expatiated in carbon-black-filled NR systems.²⁸ At large strain amplitudes, there are two main dissipation ways for filled rubbers: (1) the first is due to the yielding of glassy bridges: the dissipation of the stored elastic energy, and (2) the second is due to the shearing of polymer layers between the fillers, and this mechanism is present after the glassy bridges have yielded. For carbon-black-filled NR systems, the yielding of glassy bridges releases a large quantity of elastic energy, and it is converted into heat. The B_4C -filled system probably did not have such a mechanism, so the heat buildup of B_4C -filled NR was significantly lower.

CONCLUSIONS

The mechanical properties, thermal conductivities, and heat buildup of B_4C /NR composites were investigated. With the addition of B_4C , the tensile

strength was enhanced even at low and intermediate volume contents, whereas it only slightly deteriorated at high volume contents. Investigations of the nonlinear viscoelasticity and thermal conductivity of the B₄C/NR composites demonstrated that well-maintained, highly thermally conductive pathways were formed in the NR matrix, which was the main reason for the enhancement of thermal conductivity. Heat generation was significantly attenuated by the inclusion of the B₄C network for the following reasons: (1) heat was conducted away more effectively for increased thermal conductivity, and (2) a small specific area and weak interfacial activity reduced the interfacial friction remarkably.

References

1. Medalia, A. I. *Rubber Chem Technol* 1991, 64, 481.
2. Luo, R. K. *J Rail Rapid Transit* 2005, 219, 239.
3. Gehman, S. D.; Jones, P. J.; Woodford, D. E. *Ind Eng Chem* 1943, 35, 964.
4. Kar, K. K.; Bhowmick, A. K. *J Appl Polym Sci* 1996, 64, 1541.
5. Meinecke, E. *Rubber Chem Technol* 1991, 64, 269.
6. Reed, T. F. *Elastomerics* 1989, 121, 22.
7. Funt, J. M. *Rubber Chem Technol* 1988, 61, 842.
8. Gwaily, S. E.; Badawy, M. M.; Hassan, H. H.; Madani, M. *Polym Test* 2002, 21, 129.
9. Cassagnau, P. *Polymer* 2003, 44, 2455.
10. Gauthier, C.; Reynaud, E.; Vassoille, R.; Stelandre, L. L. *Polymer* 2004, 45, 2761.
11. Ramier, J.; Gauthier, C.; Chazeau, L.; Stelandre, L.; Guy, L. *J Polym Sci Part B* 2007, 45, 286.
12. Fröhlich, J.; Niedermeier, W.; Luginsland, H. D. *Compos A* 2005, 36, 449.
13. Payne, A. R.; Whittaker, R. F. *Rubber Chem Technol* 1971, 44, 440.
14. Medalia, A. I. *Rubber Chem Technol* 1978, 51, 437.
15. Payne, A. R. *J Appl Polym Sci* 1963, 7, 873.
16. Phelan, P. E.; Niemann, R. C. *J Heat Transfer* 1998, 120, 971.
17. Lin, F.; Bahtia, G. S.; Ford, J. D. *J Appl Polym Sci* 1993, 49, 1901.
18. Wood, C.; Emin, D.; Gray, P. E. *Phys Rev B* 1985, 31, 6811.
19. Garret, K. W. *J Phys D* 1974, 7, 1247.
20. Sundstrom, D. W. *J Appl Polym Sci* 1972, 16, 3159.
21. Agari, Y.; Uno, T. *J Appl Polym Sci* 1986, 32, 5705.
22. Agari, Y.; Ueda, A.; Nagai, S. *J Appl Polym Sci* 1993, 49, 1625.
23. Bruggeman, D. A. G. *Ann Phys* 1935, 24, 636.
24. Wang, J. J.; Su, Y. X. *Compos Sci Technol* 2004, 64, 1623.
25. Nan, C. W.; Liu, G.; Lin, Y. H.; Li, M. *Appl Phys Lett* 2004, 85, 3549.
26. Nan, C. W.; Birringer, R. *Phys Rev B* 1998, 57, 8264.
27. Thomas, T. C.; Gates, T. S. *Polymer* 2006, 47, 5990.
28. Merabia, S.; Sotta, P.; Long, D. R. *Macromolecules* 2008, 41, 8252.